Journal of Medicinal Chemistry

Brief Article

pubs.acs.org/jmc

Activation of C−H Bonds in Nitrones Leads to Iridium Hydrides with Antitumor Activity

Xiaoda Song,[†,∥] Yong Qian,[†,∥] Rong Ben,[†] Xiang Lu,[†] Hai-Liang Zhu,*[,†] Hui Chao,*[,§] and Jing Zhao*[,†,‡]

[†]Institute of Chemistry and BioMedical Sciences, State Key Laboratory of Pharmaceutical Biotechnology, School of Life Sciences, Nanjing University, Nanjing 210093, China

[‡]Shenzhen Key Lab of Nano-Micro Material Research, School of Chemical Biology and Biotechnology, Shenzhen Graduate School of Peking University, Shenzhen 518055, China

[§]School of Chemistry and Chemical Engineering, Sun Yat-Sen University, Guangzhou 510275, China

Supporting Information

ABSTRACT: We report the design and synthesis of a series of new cyclometalated iridium hydrides derived from the C−H bond activation of aromatic nitrones and the biological evaluation of these iridium hydrides as antitumor agents. The nitrone ligands are based on the structure of a popular antioxidant, α-phenyl-*N*-*tert*-butylnitrone (PBN). Compared to cisplatin, the iridium hydrides exhibit excellent antitumor activity on HepG2 cells. The metal-coordinated compound with the most potent anticancer activity, **2f**, was selected for further analysis because of its ability to induce apoptosis and interact with DNA. During in vitro studies and in vivo efficacy analysis with tumor xenograft models in Institute of Cancer Research (ICR) mice, complex **2f** exhibited antitumor activity that was markedly superior to that of cisplatin. Our results suggest, for the first time, that metal hydrides could be a new type of metal-based antitumor agent.

INTRODUCTION

Metal-based chemotherapy has become an important treatment option for suppressing tumor growth and inhibiting metastasis progression.[1] The design of metallodrugs is distinct from the design of traditional organic pharmacophores in that a different, sometimes unique, chemical space is accessible, with multiple coordination numbers, coordination geometries, and a large selection of ligands.[2] Considerable efforts have been focused on platinum compounds since the discovery of cisplatin, which is still one of the best-selling anticancer drugs after its approval by Food and Drug Administration in 1978 (Scheme 1).[3] However, severe side effects and drug resistance limit its applications.[3] Thus, drug design strategies, such as varying the metal center and ligands, have been employed to improve the properties of metal-based anticancer agents.[4] For example, the ruthenium complexes KP1019 and NAMI-A are currently in clinical trials (ligand-coordinated compounds are referred to as "complexes" in inorganic chemistry, and we will use this term here).[5] More recently, iridium complexes have shown potential as anticancer agents.[6] Meggers and co-workers demonstrated an octahedrally coordinated iridium(III) complex as a nanomolar-level selective inhibitor of the receptor protein kinase VEGFR3 (Flt4).[7] An iridium(III) complex with one of the strongest activity at inhibiting tumor necrosis factor-α (TNF-α) has been reported by Ma et al.[8] In addition to these two rationally designed iridium(III) complexes, other iridium-containing complexes with anticancer activity were designed to contain bulky ligands, causing significant distortions to the DNA structure.[9a,b] Several complexes containing iridium−halide bonds have been reported,[2,6c] and these covalently bind to guanine and adenine bases through N7 sites, similarly to platinum-based complexes.[9c−e]

Scheme 1. Classes of Metal-Based Drugs

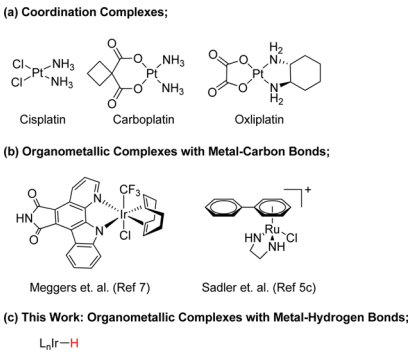

In addition to the traditional coordination complexes and organometallic complexes featuring metal−carbon bonds, we report in this manuscript the design, synthesis, and biological evaluation of a series of new iridium(III) complexes with a metal−hydrogen bond. The aromatic C−H bonds in the bidentatenitrone ligands were activated to yield the iridium hydrides. One of the products was fully characterized using NMR spectroscopic methods and X-ray analysis. The in vitro studies revealed that the complexes have strong antiproliferative effects on HepG2 cells, a human hepatocellular liver carcinoma cell line. Complex **2f**, which had the highest activity in cell culture, exhibited greater activity than cisplatin in our in vivo tumor model system. Mechanistic experiments indicated that complex **2f** has a strong interaction with DNA and induces cancer cells to generate reactive oxygen species (ROS). These

Received: April 6, 2013
Published: July 11, 2013

 © 2013 American Chemical Society

results suggest a new strategy to expand our capacity for developing new anticancer drugs.

RESULTS AND DISCUSSION

Organometallic Hydride Design and Synthesis. We selected bidentate arylnitrone ligands based on the structure of α-phenyl-*N*-*tert*-butylnitrone (PBN), which has been shown to be an effective radical scavenger and a nitric oxide donor, as well as to decrease oxidative stress.[10] PBN derivatives have also been shown to exhibit anticancer activity.[11] The synthesis of the nitrone ligands and their complexes is outlined in Scheme 2.

Scheme 2. Synthesis of the Octahedral Iridium Complexes Used in This Study

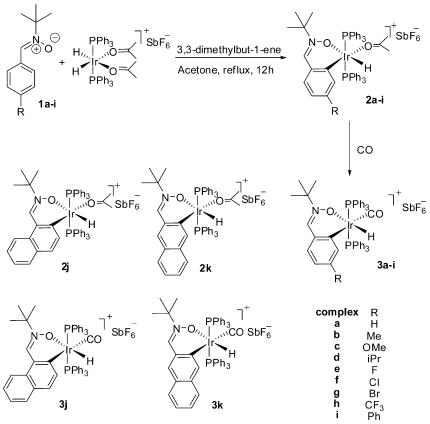

The nitrones (**1a**−**k**) are proposed to provide astronger donating oxygen than alcohols. A series of nitrones were prepared through one-pot reactions of aldehydes and *N*-*tert*-butyl hydroxylamine hydrochloride in CH_2Cl_2 with excellent yields. $[IrH_2(Me_2CO)_2(PPh_3)_2]^+$ has been shown to be effective in many catalytic reactions, including C−H activation,[12] and appears to be a reasonable choice as a starting material. The $[IrH_2(Me_2CO)_2(PPh_3)_2]SbF_6$ and the corresponding nitrone ligand were refluxed in acetone in the presence of 3,3-dimethylbut-1-ene as a hydrogen acceptor. After simple purification, the expected iridium complexes (**2a**−**k**) as the only products with good yields (Scheme 2). These products are formed via C−H bond activation and are stable toward air and moisture in both their solid and solution forms. The complex **2f** was generally stable in human microsome metabolic tests (Supporting Information (SI), pp S10−S11).

The new iridium complexes (**2a**−**k**) were fully characterized using ^1H, ^{13}C, and ^{31}P NMR spectroscopy. In the ^1H NMR spectra (acetone-d_6), complexes **2a**−**k** presented a high-field triplet resonance at δ −20 to −30, indicative of the hydrides due to their coupling to two phosphines. A single crystal of complex **2a** acetonitrile analogue suitable for structure determination by X-ray crystallography was obtained via the diffusion method (Figure 1). A crystallographic study of **2a** acetonitrile analogue revealed that the iridium complex has an octahedral geometry. The oxygen of the nitrone moieties was coordinated *trans* to the hydride and acted as a directing group to assist the activation of the ortho C−H bond via cyclometalation. The two phosphines are in a *trans* arrangement with a P(2)−Ir−P(1)angle of 176.46(6)°. The Ir−C(1)bond distance is 2.007(6) Å, and the Ir−O(1) bond distance is 2.169(5) Å.

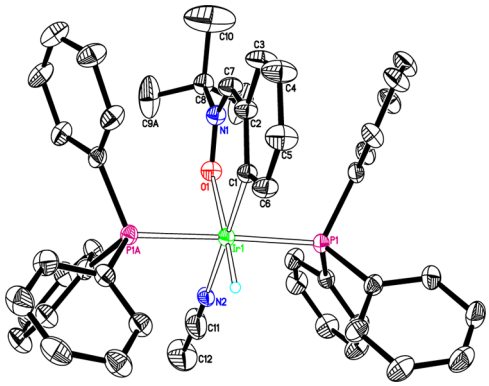

Figure 1. ORTEP representation (50% thermal ellipsoids) of the crystal structure of complex **2a** acetonitrile analogue.

Acetone ligand in complexes **2** is easily replaced by other strong-binding ligands such as acetonitrile and carbon monoxide (CO). When the acetone ligand is replaced with a carbon monoxide (CO) ligand, the CO ligand will be more likely to stay on iridium. As a comparison, iridium carbonyl complexes **3a**−**k** were prepared by bubbling CO (1 atm, 10 min) through a CH_2Cl_2 solution of complexes **2a**−**k**, resulting in the substitution of the acetone ligand (Scheme 2). The ^1H, ^{13}C, and ^{31}P NMR spectroscopic analyses were performed to confirm the formation of these complexes.

In Vitro Biological Evaluation. With the nitrone ligands (**1a**−**k**), the iridium acetone complexes (**2a**−**k**), and the iridium CO complexes (**3a**−**k**) in hand, their antiproliferative activity was evaluated by using HepG2 cells. The IC_{50} values (the drug concentration at which 50% of the cells were viable relative to the control) were calculated from the dose−survival curves, which were obtained by using the 3-(4,5-dimethylthiazol-2-yl)-2,5-diphenyltetrazolium bromide (MTT) assay after 48 h of drug treatment. The results are summarized in Table 1.

Table 1. IC_{50} Values of the Iridium Complexes 2a−k and 3a−k, Nitrone Ligands, and Cisplatin (IC_{50} ± SD(μM)) on the HepG2 Cell Line

	nitrone ligand (1)	iridium acetone complex (2)	iridiumCO complex (3)
a	>20	4.76 ± 0.4	1.26 ± 0.12
b	>20	1.85 ± 0.22	1.19 ± 0.15
c	>20	1.92 ± 0.18	1.72 ± 0.2
d	>20	1.46 ± 0.12	1.15 ± 0.08
e	>20	1.76 ± 0.14	3.07 ± 0.41
f	>20	0.82 ± 0.08	1.63 ± 0.17
g	>20	1.46 ± 0.15	2.78 ± 0.31
h	>20	1.75 ± 0.16	3.15 ± 0.36
i	>20	2.27 ± 0.24	1.12 ± 0.15
j	>20	5.03 ± 0.48	3.79 ± 0.37
k	>20	4.98 ± 0.52	3.58 ± 0.32
$[IrH_2(Me_2CO)_2(PPh_3)_2]SbF_6$		>20	
cisplatin[13]		21.55 ± 1.45	

Complex **2f** exhibited the strongest inhibitory activity, with an IC_{50} value that is approximately 26-fold lower than that of cisplatin. The nitrone ligands alone showed no significant antiproliferative activity (IC_{50} values all greater than 20 μM), indicating that the iridium−ligand complexation is essential for inhibiting HepG2 cell growth. Complex **2f** was further

investigated on NCI-60 cell lines by National Cancer Institute Developmental Therapeutics Program, and the in vitro testing results were included in the SI (Figure S3).

To investigate the cell-killing mechanism, HepG2 cells treated with a range of concentrations of **2f** were stained with DAPI, a blue nucleolar DNA staining dye. The treated cells exhibited apoptotic features, including chromatin aggregation and nucleolus fragmentation in a dose-dependent manner (SI Figure S1). To further confirm that complex **2f** induces HepG2 cells to undergo apoptosis, HepG2 cells treated with **2f** were tested using an Annexin V-FITC/propidium iodide (PI) assay. This assay is based on the translocation of phosphatidylserine from the inner leaflet of the plasma membrane to the cell surface in cells during early apoptosis. The cells in early apoptosis are in the lower right quadrant (annexin V^+PI^-), and the cells in late apoptosis are in the upper right quadrant (annexin V^+PI^+) (SI Figure S2). The culture of HepG2 cells growing in medium with the DMSO treatment contained a low number of apoptotic cells (SI Figure S2A). A significant induction of apoptosis was observed upon treatment with complex **2f** at 0.5, 1, and 1.5 μM for 48 h. The proportions of cells in late apoptosis and early apoptosis were 5.90% and 14.25%, 6.52% and 18.36%, and 7.21% and 25.17%, respectively (SI Figure S2B−D).

Mechanistic Experiments. A cell cycle analysis was performed to elucidate the mechanism of growth inhibitory activity of complex **2f** (SI Figure S8). HepG2 cells were treated with complex **2f** at a concentration of 5 μM for 48 h using the same concentration of cisplatin as the control. The cells were subsequently fixed and stained with PI, and the DNA content was analyzed by flow cytometry. Relative to the DMSO-treated control, complex **2f** caused an increase in the number of cells undergoing apoptosis (SubG1-peak), with a concomitant decrease in the number of cells in the G1, S, and G2/M phases. Furthermore, complex **2f** was more effective than cisplatin at inducing cell apoptosis (SI Figure S8). This cell cycle analysis clearly indicates that complex **2f** causes apoptosis to reduce the cell numbers.

The cell accumulation, cell fraction distribution, and DNA binding of the iridium complex **2f** in HepG2 cells were determined. The iridium contents in the whole cell, nucleus, cytosol, membrane, cytoskeleton fractions, and genome DNA were quantified (via ICP-MS, Table 2) after 24 h of exposure to complex **2f**. The amount of iridium located within genome DNA (1.8%) was similar to that of cisplatin (1%),[14] suggesting that DNA might be a potential target for these cytotoxic iridium complexes.

Table 2. Iridium Accumulation and Cell Fraction Distribution in HepG2 Cells (ng Ir/10^6 cell)

	mean	SD
cell	31.9	1.9
genome DNA	0.5	0.06
membrane	16.6	3.0
cytoskeleton	3.5	0.4
cytosol	3.9	1.6
nucleus	1.2	0.2

CD spectroscopy was performed to investigate the interaction of complex **2f** with plasmid pMD18 DNA. After incubation of DNA with complex **2f**, a significant decrease in the intensity of the positive CD band at 275 nm and the negative CD band at 245 nm was observed, suggesting that a strong interaction occurs between the DNA and complex **2f** and that DNA undergoes conformational changes due to this interaction (SI Figure S4).

Taking advantage of their unique shifts in ^{1}H NMR and ^{31}P NMR spectra, the Ir−H and Ir−P resonances could provide insights for the interaction between complex **2f** and DNA. We set out to mix complex **2f** with a segment of oligoDNA and five nucleosides (uridine, thymidine, guanosine, cytidine, and adenosine). First, we selected a synthetic oligonucleotide containing a 25-mer (5′-ATGATTTAGGTGACACTATAG-CAGT-3′), a dinucleotide (dGpG) that has been used for the cisplatin−DNA binding test.[15] After incubation of complex **2f** and the complementary double-stranded oligoDNA at 310 K for 6 h in 86% DMSO-d_6−14%D_2O, the resonance of the high-field triplet Ir−H was found to shift from −22.6 ppm to −23.94, −24.01, and −24.34 ppm. This pattern was similar to the combination of complex **2f** with adenosine (−24.07, −24.30 ppm) and cytidine (−24.04 ppm) (SI Figure S7a). In contrast, uridine and thymidine did not appear to interact with complex **2f** based on the ^{1}H NMR spectroscopy measurement (SI Figure S7a).

In addition, because there are significant amounts of iridium accumulated in the membrane (∼17%), the cell membrane could be a potential target for iridium complex **2f**. To investigate this possibility, we utilized the membrane-permeable JC-1 dye to monitor the effect of complex **2f** on the mitochondrial membrane. The JC-1 dye exhibits potential-dependent accumulation in mitochondria, indicated by a fluorescence emission shift from green (∼529 nm) to red (∼590 nm). We did not observe a significant fluorescence change after treatment with complex **2f** (SI Figure S5), suggesting that complex **2f** did not induce a decrease in the mitochondrial membrane potential.

Inspired by the recent findings that the antitumor activity of organometallic complexes may involve the redox signaling pathways in cancer cells,[16] the fluorescent probe 7-dichlorodihydrofluoresceindiacetate (DCFH-DA) was used to explore the possible generation of cellular ROS with the introduction of an iridium complex. The green fluorescence was detected over a period of 4 h after treating the cells with complex **2f** (5 μM) (SI Figure S6). The ROS generation capacity of complex **2f** was found to be stronger than that of 12 μM H_2O_2.

In Vivo Biological Evaluation. On the basis of these in vitro studies, complex **2f** was used to examine its effect on in vivo xenograft models in ICR mice. The tumor xenograft nodules were formed by subcutaneous injection of H22 cells. The mice were then treated with complex **2f** at a dose of 3 mg/kg by intraperitoneal injection, and cisplatin was used as a control for comparison with the antitumor efficiency in the xenograft model. Figure 2a shows the change in tumor volume by intraperitoneal administration in H22 cells via the xenograft tumor in mice. Both cisplatin and complex **2f** effectively inhibited tumor growth. The tumor volumes in the control group receiving saline increased rapidly from day 6, with their mean tumor volumes reaching more than 4000 mm^3 on day 24. In comparison, groups receiving either cisplatin or complex **2f** showed retardation in tumor growth, with the mean tumor volumes near 1000 mm^3 on day 24. Importantly, complex **2f** showed at least the same level of efficacy in inhibiting tumor growth compared to that of cisplatin. Statistical analysis revealed that the cohort receiving the treatment with complex

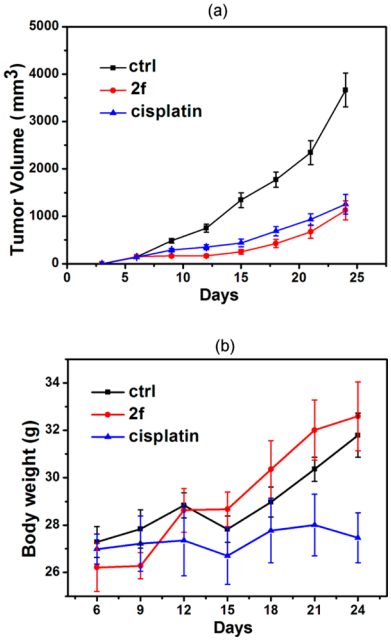

Figure 2. In vivo efficacy of complex **2f** against H22 tumor cells in ICR mice. (a) Tumor volume established in ICR mice during therapy under different treatments. (b) Body weight change of ICR mice receiving different treatments during therapy. Data are presented as the mean body weight ± SD (n = 6).

2f had similar tumor volumes compared to the cisplatin-treated group from day 9 to day 24.

To determine the adverse effects of these therapeutic treatments, we analyzed the variations in body weights during these experiments. The complex **2f**-treated group showed favorable results without any obvious loss of body weight, whereas treatment with cisplatin led to severe weight loss in the mice (Figure 2b). The in vivo efficacy results were consistent and correlated well with the data obtained from in vitro cell culture analyses, indicating that complex **2f** exhibits an anticancer activity that is better than that of cisplatin. When healthy mice were treated with complex **2f**, no noticeable weight loss was observed (SI Figure S8).

CONCLUSION

In conclusion, we report the synthesis of iridium hydrido complexes (**2a**−**k**) and iridium hydrido CO complexes (**3a**−**k**) with aromatic nitrones (PBN) as ligands (**1a**−**k**). Biological evaluation of the antitumor activity of these ligands (**1a**−**k**) and their iridium complexes (**2a**−**k**, **3a**−**k**) indicated that these iridium hydrides exhibited excellent antitumor activity on tumor cells. The complex with the most potent antitumor activity, **2f**, was selected for further screening using NCI-60 cell lines and exhibited promising activity. Further analysis confirmed its ability to induce apoptosis. Preliminary mechanistic studies revealed a strong interaction between the iridium complex **2f** and DNA. Finally, complex **2f** was shown to be effective in vivo using tumor xenograft models in ICR mice, exhibiting less toxicity than that of cisplatin. Previous research on metal hydrides has mainly focused on their catalytic roles, especially in the area of C−H bond activation. Numerous metal hydrides have been obtained from intensive research on C−H bond activation. We expect that our findings could open doors to further investigation of the biological activities of metal hydrides.

EXPERIMENTAL SECTION

General Methods for Synthesis. Unless otherwise mentioned, all manipulations were performed using standard Schlenk techniques; all reagents were purchased from commercial suppliers without any further purification, and all solvents were distilled before use unless otherwise noted. Nuclear magnetic resonance (NMR) spectra were acquired on Bruker DRX-500/300 operating at 125 and 75 MHz for ^{1}H NMR and ^{13}C NMR, respectively. All ^{1}H NMR spectra are reported in δ units, parts per million (ppm) downfield from tetramethylsilane as the internal standard, and the coupling constants are indicated in hertz (Hz). The following abbreviations are used for spin multiplicity: s = singlet, d = doublet, t = triplet, q = quartet, m = multiplet, and br = broad. ESI-MS spectra were recorded on a Mariner System 5304 mass spectrometer. TLC was performed on glass-backed silica gel sheets (silica gel HG/T2354-92 GF254) and visualized under UV light (254 nm). Column chromatography was performed using silica gel (200−300 mesh), eluting with ethyl acetate and petroleum ether. The purity of all compounds was >95% prior to biological testing and was determined by ultrahigh pressure liquid chromatography (Waters ACQUITY UHPLC).

*General Method for the Synthesis of **1a**−**k**.* A mixture of aldehydes (1.59 mmol), *N*-(*tert*-butyl) hydroxylamine hydrochloride (200 mg, 1.59 mmol), Na_2SO_4 (678 mg, 4.77 mmol), and $NaHCO_3$ (401 mg, 4.77 mmol) were added to CH_2Cl_2 (10 mL), and the reaction mixture was stirred and refluxed for approximately 48 h. The resulting mixture was filtered, and the solvent was then removed under vacuum. The target products (**1a**−**k**) were purified by column chromatography (silica gel, petroleum ether/ethyl acetate 3/1−1/1).

*General Method for the Synthesis of Iridium Acetone Complexes **2a**−**k**.* Under an argon atmosphere, a 25 mL Schlenk tube was charged with *N*-*tert*-butyl-α-phenylnitrone (0.31 mmol, 1.1 equiv), 3,3-dimethylbut-1-ene (1.5 mL), $IrH_2(PPh_3)_2(C_3H_6O)_2SbF_6$ (300 mg, 0.28 mmol), and dry acetone (6 mL). The mixture was stirred under reflux for 12 h. The solvent was removed, and the residue was washed with diethyl ether or pentane to obtain complexes **2a**−**k**.

*General Method for the Synthesis of Iridium CO Complexes **3a**−**k**.* An iridium acetone complex (100 mg) was dissolved into CH_2Cl_2 (6 mL) in a Schlenk tube then bubbled into carbon monoxide gas for approximately 10 min. The solvent was subsequently removed, and the residue was washed with diethyl ether or pentane to obtain complexes **3a**−**k**.

ASSOCIATED CONTENT

Supporting Information

Morphological analysis, annexin V/propidium iodide staining, MTT assay, NCI-60 cell lines test, CD, ICP-MS, UHPLC diagram crystal structure, and spectral data of MS, ^{1}H NMR, ^{13}C NMR, and ^{31}P NMR. This material is available free of charge via the Internet at http://pubs.acs.org.

AUTHOR INFORMATION

Corresponding Author

*Phone: +86 0755 2603 3151. Fax: +86 0755 2603 3174. E-mail: jingzhao@nju.edu.cn.

Author Contributions

‖X.S. and Y.Q. contributed equally.

Notes

The authors declare no competing financial interest.

ACKNOWLEDGMENTS

This work is financially supported by grants of the National Basic Research Program of China (2010CB923303 to J.Z.) and the Jiangsu Natural Science Foundation (BK2011547 to J.Z.). J.Z. thanks the Shenzhen Government (SW201110018, JC201104210113A, KQC201105310016A) for support. We

thank the National Cancer Institute Developmental Therapeutics Program for the in vitro testing results of complex **2f**.

■ ABBREVIATIONS USED

PBN, α-phenyl-*N*-*tert*-butylnitrone; ICR mice, Institute of Cancer Research mice; VEGFR, vascular endothelial growth factors receptor; (TNF-α), tumor necrosis factor-α; HepG2, hepatocellular carcinoma cell line; ROS, reactive oxygen species; MTT, 3-(4,5-dimethylthiazol-2-yl)-2,5-diphenyltetrazolium bromide; DAPI, 4′,6-diamidino-2-phenylindole; PI, propidium iodide; FITC, fluorescein isothiocyanate; JC-1, 5,5′,6,6′-tetrachloro-1,1′,3,3′-tetraethyl-imidacarbocyanine iodide; DCFH-DA, dichlorodihydrofluorescein diacetate

■ REFERENCES

(1) (a) Brabec, V. DNA modifications by antitumor platinum and ruthenium compounds: their recognition and repair. *Prog. Nucleic Acid Res. Mol. Biol.* **2002**, *71*, 1−68. (b) Clarke, M. J. Ruthenium metallopharmaceuticals. *Coord. Chem. Rev.* **2003**, *236*, 209−233. (c) Keppler, B., Ed. *Metal Complexes in Cancer Chemotherapy*; VCH, Weinheim, Germany; New York, 1993. (d) Hartinger, C. G.; Dyson, P. J. Bioorganometallicchemistry—from teaching paradigms to medicinal applications. *Chem. Soc. Rev.* **2009**, *38*, 391−401. (e) Hartinger, C. G.; Metzler-Nolte, N.; Dyson, P. J. Challenges and opportunities in the development of organometallic anticancer drugs. *Organometallics* **2012**, *31*, 5677−5685.

(2) Wirth, S.; Rohbogner, C. J.; Cieslak, M.; Julia, K. B.; Donevski, S.; Nawrot, B.; Lorenz, I. P. Rhodium(III) and iridium(III) complexes with 1,2-naphthoquinone-1-oximate as a bidentate ligand: synthesis, structure, and biological activity. *J. Biol. Inorg. Chem.* **2010**, *15*, 429−440.

(3) (a) Wong, E.; Giandomenico, C. M. Current status of platinum-based antitumor drugs. *Chem. Rev.* **1999**, *99*, 2451−2466. (b) Guo, Z.; Sadler, P. J. Metals in medicine. *Angew. Chem., Int. Ed. Engl.* **1999**, *38*, 1512−1531. (c) Ho, Y. P.; AuYeung, S. C. F.; To, K. K. W. Platinum-based anticancer agents: innovative design strategies and biological perspectives. *Med. Res. Rev.* **2003**, *23*, 633−655.

(4) Bruijnincx, P. CA.; Sadler, P. J. Controlling platinum, ruthenium, and osmium reactivity for anticancer drug design. *Curr. Opin. Chem. Biol.* **2008**, *12*, 197−206.

(5) (a) Sava, G.; Bergamo, A. \Ruthenium-based compounds and tumour growth control. *Int. J. Oncol.* **2000**, *17*, 353−365. (b) Galanski, M.; Arion, V. B.; Jakupec, M. A.; Keppler, B. K. Recent developments in the field of tumor-inhibiting metal complexes. *Curr. Pharm. Des.* **2003**, *9*, 2078−2089. (c) Habtemariam, A.; Melchart, M.; Fernandez, R.; Parsons, S.; Oswald, I. D. H.; Parkin, A.; Fabbiani, F. P. A.; Davidson, J. E.; Dawson, A.; Aird, R. E.; Jodrell, D. I.; Sadler, P. J. Structure−activity relationships for cytotoxic ruthenium(II) arene complexes containing *N,N*-, *N,O*-, and *O,O*-chelating ligands. *J. Med. Chem.* **2006**, *49*, 6858−6868. (d) Hartinger, C. G.; Jakupec, M. A.; Zorbas-Seifried, S.; Groessl, M.; Egger, A.; Berger, W.; Zorbas, H.; Dyson, P. J.; Keppler, B. K. KP1019, a new redox-active anticancer agent—preclinical development and results of a clinical phase I study in tumor patients. *Chem. Biodiversity* **2008**, *5*, 2140−2155.

(6) (a) Lau, J. S.; Lee, P. K.; Tsang, K. H.; Ng, C. H.; Lam, Y. W.; Cheng, S. H.; Lo, K. K. Luminescent cyclometalated iridium(III) polypyridine indole complexes—synthesis, photophysics, electrochemistry, protein-binding properties, cytotoxicity, and cellular uptake. *Inorg. Chem.* **2009**, *48*, 708−718. (b) Amouri, H.; Moussa, J.; Renfrew, A. K.; Dyson, P. J.; Rager, M. N.; Chamoreau, L. M. Discovery, structure, and anticancer activity of an iridium complex of diselenobenzoquinone. *Angew. Chem., Int. Ed. Engl.* **2010**, *49*, 7530−7533. (c) Liu, Z.; Habtemariam, A.; Pizarro, A. M.; Fletcher, S. A.; Kisova, A.; Vrana, O.; Salassa, L.; Bruijnincx, P. C.; Clarkson, G. J.; Brabec, V.; Sadler, P. J. Organometallic half-sandwich iridium anticancer complexes. *J. Med. Chem.* **2011**, *54*, 3011.

(7) Wilbuer, A.; Vlecken, D. H.; Schmitz, D. J.; Kräling, K.; Harms, K.; Bagowski, C. P.; Meggers, E. Iridium complex with antiangiogenic properties. *Angew. Chem., Int. Ed. Engl.* **2010**, *49*, 3839−3842.

(8) Leung, C. H.; Zhong, H. J.; Yang, H.; Cheng, Z.; Chan, D. S.; Ma, V. P.; Wong, C. Y.; Ma, D. L. A metal-based inhibitor of tumor necrosis factor-α. *Angew. Chem., Int. Ed. Engl.* **2012**, *51*, 9010−9014.

(9) (a) Schafer, S.; Sheldrick, W. S. Coligand tuning of the DNA binding properties of half-sandwich organometallic intercalators: influence of polypyridyl (pp) and monodentate ligands (L = Cl, $(NH_2)_2CS$, $(NMe_2)_2CS$) on the intercalation of (g5-pentamethylcyclopentadienyl)-iridium(III)- dipyridoquinoxaline and -dipyridophenazine complexes. *J. Organomet. Chem.* **2007**, *692*, 1300−1309. (b) Schmitt, F.; Govindaswamy, P.; Süss-Fink, G.; Ang, W. H.; Dyson, P. J.; Jeanneret, L. J.; Therrien, B. Ruthenium porphyrin compounds for photodynamic therapy of cancer. *J. Med. Chem.* **2008**, *51*, 1811−1816. (c) Sherman, S. E.; Gibson, D.; Wang, A.; Lippard, S. J. Crystal and molecular structure of *cis*-Pt[$(NH_3)_2${d(pGpG}], the principal adduct formed by *cis*-diamminedichloroplatinum(II) with DNA. *J. Am. Chem. Soc.* **1988**, *110*, 7368−7738. (d) Huang, H.; Zhu, L.; Reid, B. R.; Drobny, G. P.; Hopkins, P. B. Solution structure of a cisplatin-induced DNA interstrand cross-link. *Science* **1995**, *270*, 1842−1844. (e) Wang, D.; Lippard, S. J. Cellular processing of platinum anticancer drugs. *Nature Rev. Drug Discovery* **2005**, *4*, 307−320.

(10) Bernotas, R. C.; Thomas, C. E.; Carr, A. A.; Nieduzak, T. R.; Adams, G.; Ohlweiler, D. F.; Hay, D. A. Synthesis and radical scavenging activity of 3,3-dialkyl-3,4-dihydro-isoquinoline 2-oxides. *Bioorg. Med. Chem. Lett.* **1996**, *6*, 1105−1110.

(11) (a) Nakae, D.; Kishida, H.; Enami, T.; Konishi, Y.; Hensley, K. L.; Floyd, R. A.; Kotake, Y. Effects of phenyl *N*-*tert*-butyl nitrone and its derivatives on the early phase of hepatocarcinogenesis in rats fed a choline-deficient, L-amino acid-defined diet. *Cancer Sci* **2003**, *94*, 26−31. (b) Floyd, R. A.; Kopke, R. D.; Choi, C. H.; Foster, S. B.; Doblas, S.; Towner, R. A. Nitrones as therapeutics. *Free Radical Biol. Med.* **2008**, *45*, 1361−1374. (c) Floyd, R. A.; Towner, R. A.; Wu, D.; Abbott, A.; Cranford, R.; Branch, D.; Guo, W. X.; Foster, S. B.; Jones, I.; Alam, R.; Moore, D.; Allen, T.; Huycke, M. Anti-cancer activity of nitrones in the ApcMin/+ model of colorectal cancer. *Free Radical Res.* **2010**, *44*, 108. (d) Floyd, R. A.; Chandru, H. K.; He, T.; Towner, R. Anti-cancer activity of nitrones and observations on mechanism of action. *Anticancer Agents Med. Chem.* **2011**, *11*, 373−379.

(12) Crabtree, R. H.; Parnell, C. P. Arene and cyclohexadienyl complexes as intermediates in the selective catalytic dehydrogenation of cyclohexenes to arenes. *Organometallics* **1985**, *4*, 519−523.

(13) The IC_{50} is very close to the results reported in Sbovata, S. M.; Bettio, F.; Mozzon, M.; Bertani, R.; Venzo, A.; Benetollo, F.; Michelin, R. A.; Gandin, V.; Marzano, C. Cisplatinum and transplatinum complexes with benzyliminoether ligands: synthesis, characterization, structure−activity relationships, and in vitro and in vivo antitumor efficacy. *J. Med. Chem.* **2007**, *50*, 4775−4784.

(14) Jung, Y.; Lippard, S. J. Direct cellular responses to platinum-induced DNA damage. *Chem. Rev.* **2007**, *107*, 1387−1407.

(15) Bosea, R. N.; Maurmann, L.; Mishur, R. L.; Yasui, L.; Gupta, S.; Grayburn, W. S.; Hofstetter, H.; Salley, T. Non-DNA-binding platinum anticancer agents: cytotoxic activities of platinum−phosphato complexes towards human ovarian cancer cells. *Proc. Natl. Acad. Sci. U. S. A.* **2008**, *105*, 18314−18319.

(16) (a) Fu, Y.; Romero, M. J.; Habtemariam, A.; Snowden, M. E.; Song, L.; Clarkson, G. J.; Qamar, J.; Pizarro, A. M.; Unwin, P. R.; Sadler, P. J. The contrasting chemical reactivity of potent isoelectronic iminopyridine and azopyridineosmium(II) arene anticancer complexes. *Chem. Sci.* **2012**, *3*, 2485−2494. (b) Betanzos-Lara, S.; Liu, Z.; Habtemariam, A.; Pizarro, A. M.; Qamar, B.; Sadler, P. J. Organometallic ruthenium and iridium transfer-hydrogenation catalysts using coenzyme NADH as a cofactor. *Angew. Chem., Int. Ed.* **2012**, *51*, 3897−3900.